Experimental setup

Abstract. Chapters 3 and 4 already describe the experimental setup, not in details. This section is meant to cover details that were left out in those two articles. The setup has been also described in details in the PhD thesis of Reijnders [1] and Taban [2].
The experimental setup is schematically drawn in figure 1. The ions are created in the
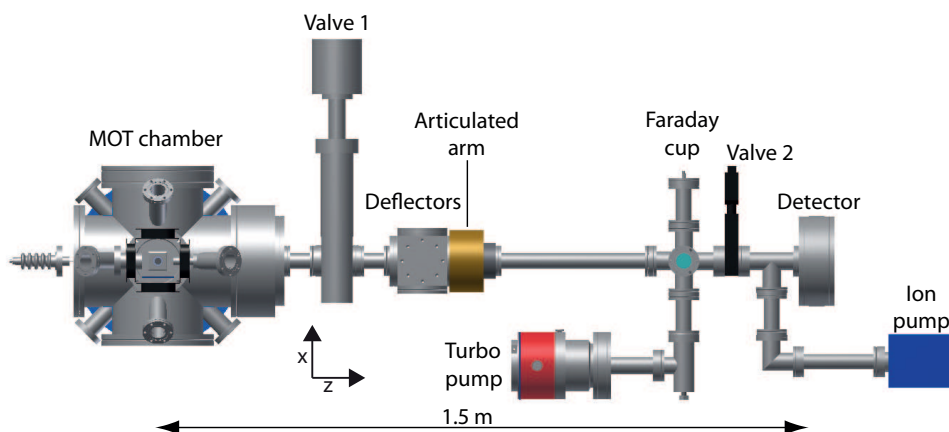
Figure 1. Schematic drawing of the beam line.

magneto-optical trap (MOT) chamber on the left hand side of the figure at $z = 0$ and travel about 1.5 m in the beam line until the detector on the right hand side. The MOT chamber is discussed in section 2. The first valve is meant to keep the MOT chamber independent from the beam line, when it is eventually not under vacuum. A couple of deflector plates are used to steer the beam in the x and directions. An articulated feature, right after the beam line permits to move the beam line up to the the detector within an angle of about $5°$. A Faraday cup can be inserted in the beam line and with the use of an electrometer, it can measure the charge of ion bunches. The detector setup and the required calibration are discussed in section 3.

1. Laser

Lasers form an important part of the setup. They are needed at first to cool down the atoms and, together with a magnetic field, to form a MOT. Also, they are used to ionize the cooled atoms. The relevant hyperfine energy levels of ^{85}Rb is plotted in
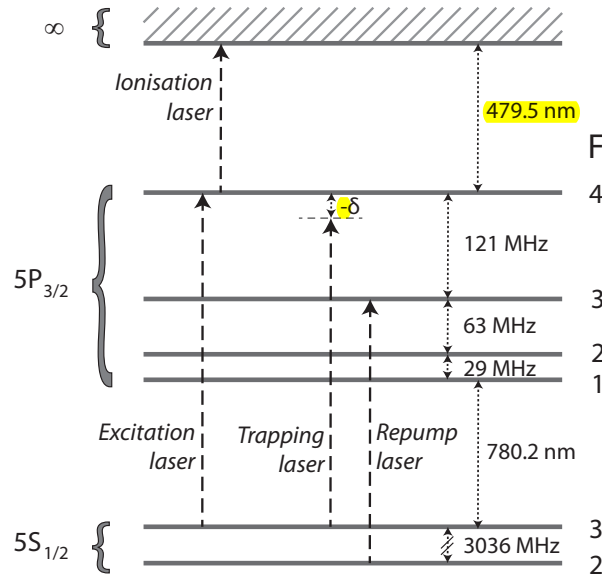
Figure 2. The relevant hyperfine energy levels of ^{85}Rb and the used laser transitions, edited from [3]. The continuum marked by ∞ is the ionized state.

figure 2, where the used laser transitions are also presented. Four different lasers are used in the lab and their properties are summarized in table 1. 1. The atoms that are

Table 1. Lasers used in the experiments.

Laser	Used as	Power / Energy	Pulse length
Toptica DLX 110	Trapping laser	900 mW	CW
Toptica DL 100	Repump laser	100 mW	CW
Quanta-Ray PDL3	ionization laser	0.1 mJ	2.5 ns *rms*
Toptica TA-SHG 110	ionization laser	250 mW	CW

trapped in the MOT, are continuously excited by the trapping laser to the $5P_{3/2}$,F=4 state, and then decay back to the $5S_{1/2}$,F=3 ground state. However, since the hyperfine levels are not that far apart, some of the trapping laser power will actually excite the transition to the $5P_{3/2}$,F=3 state. These atoms can than decay to the "wrong" ground state $5S_{1/2}$,F=2. In order to make sure that these atoms do not get pumped to that state, a repump laser is needed. This pumps the atoms back to the $5P_{3/2}$,F=3 state, from where they can also decay to the "right" ground state, $5S_{1/2}$,F=3. The repump laser is left on all time. The trapping and repump laser need to be stabilized to within a few megahertz and more details about the laser locking can be found in [1].

The difference in frequency between the trapping laser and excitation laser is very small ($\Delta f = -14.5$ MHz), therefore a single laser is used for both transitions. Moreover, the laser power needed for the excitation laser beam is only a small fraction of that needed for the trapping laser beams since the trapping laser beams are much larger

than the excitation laser beam. The trapping laser beams carry 250 mW of laser power in total, while the excitation laser beam uses at most only 10 mW of it. The detuning and intensity of the excitation and trapping laser beams are controlled using AOMs, which in turn are computer controlled by a programmable pattern generator (PPG). The PPG has an internal clock that operates at 50 MHz, so its resolution is 20 ns.

The ionization transition is that of the excited atoms from any of the $5P_{3/2}$ states to just above the ionization threshold. Note that atoms can only be ionized if are first excited. For the experiment presented in this thesis, the CW ionization laser is used. The pulsed dye laser is used as an ionization laser only in the calibration of the MCP, see section 3. The continuous ionization laser beam can be switched on and off with an acoustic-optical deflector (AOD), which are also computer controlled.

The photo-ionization takes place in the small region of the atom cloud where both the excitation laser and ionization laser are present, the core region. The trapping lasers are turned off during the ionization, in order not to excite the entire atom cloud. The size of the excitation and ionization laser beams determines the volume of this region. The laser beam sizes are measured using two cameras virtually positioned in the center of the MOT. The camera images of the laser beam profile are fitted with a 2D-Gaussian. For both laser beams the fits result in 2 rms-radii. The laser beam size combines in the x-direction as

$$\sigma_{comb} = \sqrt{\frac{\sigma_{e,x}^2 \sigma_{i,x}^2}{\sigma_{e,x}^2 + \sigma_{i,x}^2}}, \tag{1}$$

and the core volume is $(\sigma_x, \sigma_y, \sigma_z) = (\sigma_{comb}, \sigma_{e,y}, \sigma_{i,z})$. The quantities $\sigma_{i,x}$ and $\sigma_{i,z}$ are the fitted rms-radii of the ionization laser in respectively the x and z-direction, $\sigma_{e,x}$ and $\sigma_{e,y}$ are the fitted rms-radii of the excitation laser in respectively the x and y-direction, and σ_{comb} is the combined rms-radius in the x-direction.

2. Magneto-optical trap

The MOT is located in a vacuum chamber, where the typical pressure is below 10^{-8} mbar. A schematic representation of the vacuum chamber can be found in figure 3. The trapping laser beams are three orthogonal pairs of counter-propagating circularly polarized, intersecting in the center of the trap. A magnetic field is generated by two coils placed in an anti-Helmholtz configuration, resulting in a field gradient of about 1 G/mm. The trapping beams together with the magnetic field gradient slow down and trap the atoms in the center of the MOT. The atoms will form a cloud with a *rms*-radius of about 1 mm.

As the trapping lasers continuously excite the trapped atoms, they send out spontaneously emitted photons. Two CCD cameras observe the fluorescence of the MOT, one from the top and one from the side, continuously determining the density and the dimension of the MOT [4].
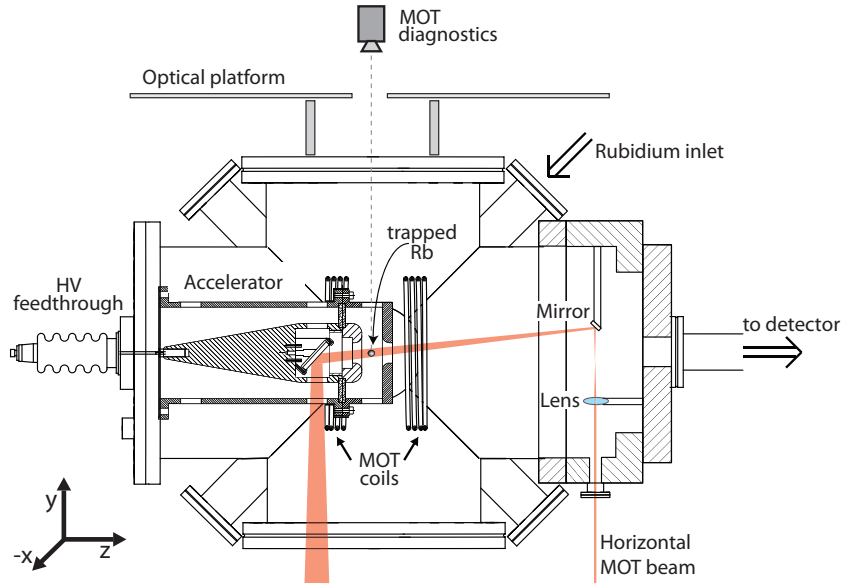
Figure 3. Schematic overview of the vacuum chamber that contains the MOT and accelerator structure [2]. One of the trapping laser beam pairs is shown, namely the horizontal beam pair. This pair consists of two separate laser beams, which are reflected by mirrors before they reach the MOT. It is not exactly horizontal, because in that case the mirror on the right would block the outcoming ion beam. The other pairs are diagonal beams in the (x, y)-plane, which are back-reflected. The coils that create the magnetic field gradient are also indicated in the figure. Finally, there are two cameras observing the fluorescence of the MOT, only the top one is shown. The side camera is behind the setup, looking toward the reader.

3. Calibration of the MCP detector

A scheme of the detector is shown in figure 4. In front of the detector there is a grounded
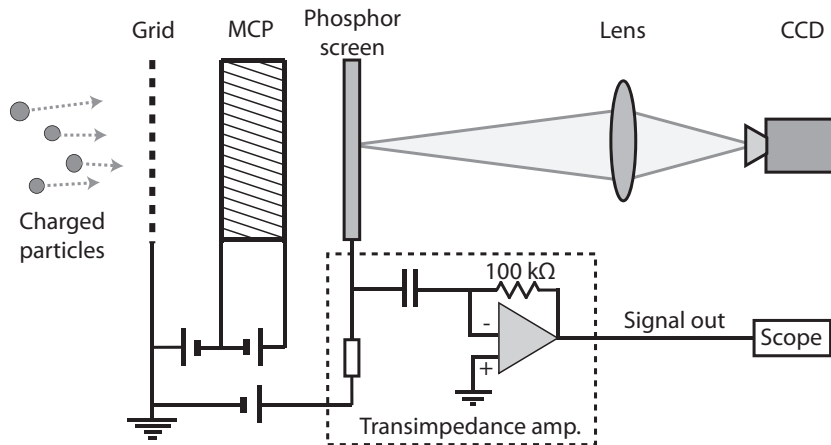

Figure 4. Schematic illustration of the MCP detector assembly with phosphor screen. A grounded grid is used to shield the electric field of the MCP in the beam line. A trans-impedence amplifier is used to conver the current signal to a voltage signal, readable with an oscilloscope.

metal grid, used to shield the ions in the beam-line from the field generated by the detector. This grid has a 50% open area, so only about half of the created ions will reach the detector. The detector is a double micro-channel plate (MCP), manufactured by Photonis, that consists of two 40 mm diameter glass plates. These plates contain millions of glass channels with a radius of 5 μm, distanced 8 μm apart. The channels are placed at a 5 degrees angle with respect to the z-axis. Ions colliding with the MCP can create a secondary electron, which gets accelerated by the potential difference over the MCP. When these electrons have accumulated enough energy and they collide again with the wall, an extra secondary electron can be emitted, so that, effectively, the MCP acts as a charge multiplier. The created electrons are accelerated towards a phosphor screen, which emits light at the position where the electron bunch hits it. This light is captured by a CCD camera and the camera images can be analyzed to determine the spatial distribution of the ions. The corresponding electron current is converted to a voltage by a trans-impedance amplifier, schematically contained in the figure 4. Effectively both inputs of the operational amplifier (opamp) get the same potential, in this case 0 V. The current runs through the resistor. Therefore the output voltage of the circuit is $V_{ti} = -I \cdot 0$ kΩ. Because electrons flow opposite to the current, a positive voltage is created, which is measured with an oscilloscope.

Before any absolute current measurements can be performed, the micro-channel plate (MCP) needs to be calibrated. This calibration involves determining the ratio between the electron current that arrives at the phosphor screen and the ion current arriving at the MCP. The used calibration method consists of several steps: the main idea is to determine the average charge per pulse and the average output signal. This involves averaging over many ionization cycles to get rid of fluctuations in the signal. Such fluctuations are not only caused by noise, but also by the randomness of the ionization process itself: all atoms in the ionization volume have a probability to be ionized. Also, the actual number of atoms in the ionization volume fluctuates over time. Finally, the power of especially the pulsed dye laser varies quite drastically from pulse to pulse. By averaging, the fluctuations become relatively small, and an accurate calibration can be done. In order to have an idea of the size of the remaining fluctuations, the first two experiments that use the pulsed laser (operating at only 10 Hz) are performed twice.

The first step is to determine the amount of charge that arrives at the MCP. In this experiment the MCP is actually used as a Faraday cup, which basically is a charge collector that is placed in the beam. This is achieved by connecting the phosphor screen with the rear end of the MCP, and applying a small positive voltage of 50 V on the front end of the MCP. This small positive voltage does not significantly affect the incoming ions, which have a much higher energy (between 0.8 and 3 keV), but does make sure that no secondary electrons escape from the MCP. Since the phosphor screen and rear of the MCP are both a floating connection there will be no voltage difference over the MCP, so that no charge amplification takes place.

The ions are generated using a pulsed dye laser, which has a pulse length of about 5 ns and a repetition rate of 10 Hz. Hence, all of the ions will be created in a very short time frame. They are accelerated towards the MCP using the maximal acceleration voltage, $V_a = 6$ kV, so that the ion bunch stays as compact as possible. Nevertheless, it expands to a size larger than the MCP. The advantage of this is that the entire MCP is used, so that the current does not saturate the detector. The obvious disadvantage is that the total charge arriving at the MCP is lower than the ionized one. Hence, the signal obtained by measuring the current through the connector of the front of the MCP, needs to be amplified. This current is amplified with a pre-amplifier and a shaping amplifier. The shaping amplifier is used to generate a bipolar pulse and is used with a gain of 1000 and a shaping time of 10 μs, which is much longer than the length of the ion pulse. Because of this the peak-to-peak output of the shaping amplifier is a measure for the charge that arrived at the MCP. This combination of pre-amplifier and shaping amplifier has been separately calibrated and gives an amplification factor of 1.23 fC/V for a gain of 1000 [5]. In figure 5, the output of the shaping amplifier is plotted versus time. Each line corresponds to the average over 1024 consecutive ion bunches. The experiment has been performed twice to get an idea of the reproducibility of the measurement. As it turns out, the two experiments agree very well, so that the charge for this experiment is determined to be 1.17 ± 0.02 fC.

Within ten minutes of the charge determination, a voltage difference is applied over the
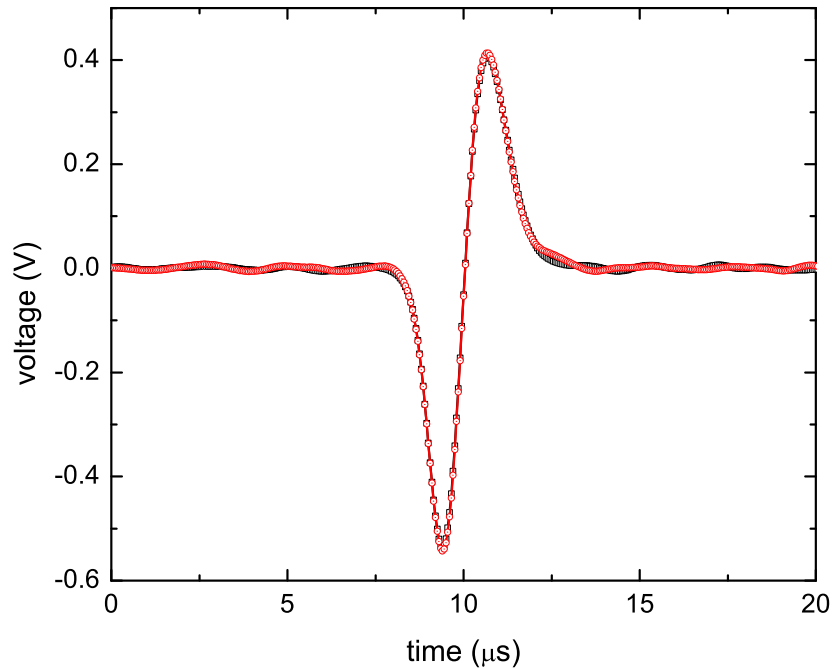

Figure 5. Bipolar output of the shaping amplifier. The peak-to-peak voltage is proportional to the total charge in the pulse. Two lines are plotted, both of which are the average of 1024 consecutive ion bunches. The peak-to-peak voltages agree, so the average charge has been determined quite accurately to be 1.17 ± 0.02 fC.

MCP plates, so that it will act as a charge multiplier again. The applied voltage at the

front of the MCP is $V_{in} = -1550$ V, while the rear of the MCP is at $V_{out} = 0$ V. The phosphor screen is at a positive voltage of $V_{ph} = 1000$ V. ~~Again,~~ the ~~measured~~ voltage is averaged over 1024 consecutive ion bunches and performed twice. The results are plotted in figure 6. In this case, there is some disagreement between the two measurements. This can be caused by a relatively small increase of the voltage over the MCP: a difference of only 7 V in terms of $\Delta_{MCP} = V_{out} - V_{in}$ could explain the change. This is in accordance with the voltage-stability of the high voltage supplies used to power the MCP. Hence, the minimal error margin of the current measurements is 10%. The signal needs to be integrated over time to get the charge of the bunch, which ~~is~~ on average (4.0 ± 0.2) μV s. This corresponds to a charge of 40 ± 2 pC ~~(100 kΩ)~~ and hence a MCP gain of $(34 \pm \boxed{}) 10^3$.
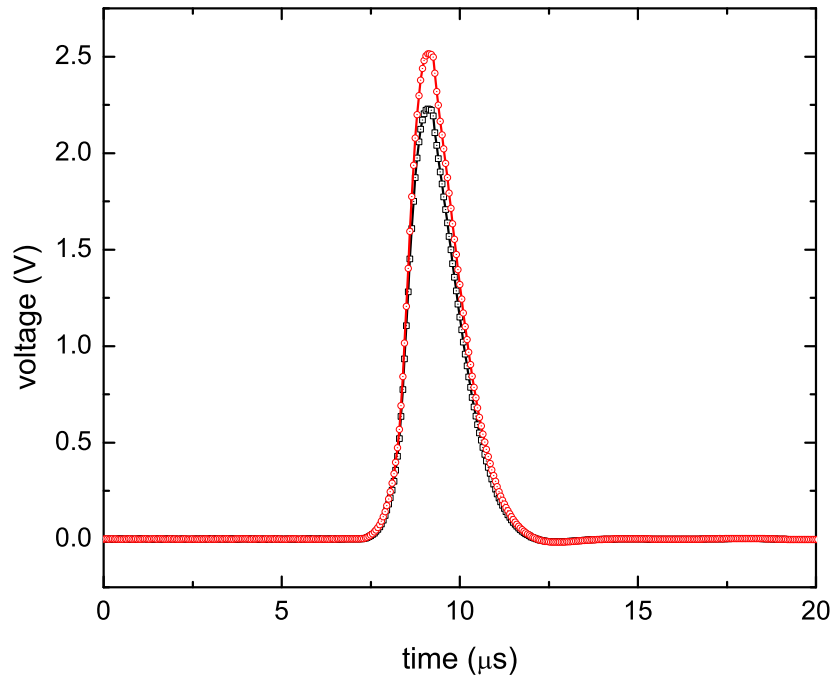

Figure 6. The output of the trans-impedance amplifier, during the calibration measurement, where the different colors correspond to two identical series taken after each other. The duration of the peak is si$\boxed{}$ to that of the ionization laser pulse.

This calibration can be used to relatively calibrate the MCP for other acceleration voltages and MCP potential differences ~~as.~~ This is performed with Δ_{MCP} being 1500 V, 1600 V, 1650 V, 1700 V, 1750 V. The results of these experiments are plotted in figure 7, which shows the gain of the MCP, plotted on a logarithmic scale, as a function of the voltage over the MCP, for an acceleration voltage $V_a = 800$ V. As can be seen the gain increases almost exponentially with the voltage. This exponential relationship (fitted through the first two points) has also been plotted as a dashed line. For higher voltages over the MCP a saturation effect occurs.
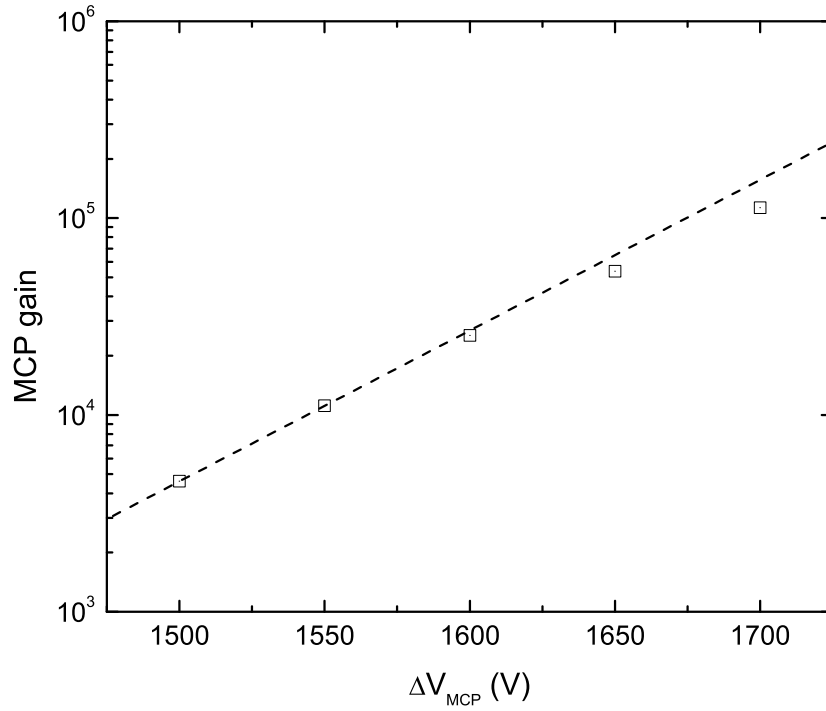
Figure 7. The gain as determined by the calibration experiments for an acceleration energy $V_a = 800$ V which correspond to a beam energy of about 400 eV. All points have a systematic error of about 10%. The dashed line corresponds to an exponential increase of the gain, fitted through the first two points.

4. Calibration of the CCD camera

A CCD camera is used to image the phosphor screen through a lens placed in between with a magnification of 0.33. The spatial distribution of the ion bunches can be extracted from the CCD images. The resolution of the detector has been determined experimentally by placing two pinholes, with diameters $2r_p$ of 25 μm and 50 μm, downstream in front of the MCP. Ion bunches with $U = 3$ keV passed through one of the two pinholes at a time. The *rms*-radius σ_a of an aperture with radius a is given by

$$\sigma_a = \sqrt{\frac{\int dx \; x^2 \sqrt{r_p^2 - x^2}}{\int dx \sqrt{r_p^2 - x^2}}} = \frac{r_p}{2}, \tag{2}$$

The *rms* spot radius σ_{det} measured at the detector was substantially larger than σ_a, as a result of the resolution of the detector. Multiple experiments, with both the pinholes, have been performed in order to obtain sufficient statistical accuracy. Using

$$\sigma_{det} = \sqrt{\delta^2 + \sigma_a^2}, \tag{3}$$

the *rms* resolution of the detector δ is found to be (95 ± 4) μm.

[1] M. P. Reijnders. *Ion beams from laser-cooled gases.* PhD thesis, Eindhoven University of Technology, 2010.

[2] G Taban. *A cold atom electron source.* PhD thesis, Eindhoven University of Technology, 2009.

[3] B. J. Claessens. *Dynamics and Applications of Excited Cold Atoms.* PhD thesis, Eindhoven Technological University, 2006.

[4] K.H.M. Hermans. *Measurement and modeling of Ultra Cold Ion current pulses.* Bachelor's thesis, Eindhoven Technological University, 2010.

[5] M.A. van der Heijden. Creation and characterization of ultrashort ultracold electron bunches. Master's thesis, Eindhoven Technological University, 2011.